J Neurophysiol 120: 1374–1385, 2018.
First published June 27, 2018; doi:10.1152/jn.00158.2018.

RESEARCH ARTICLE | *Cellular and Molecular Properties of Neurons*

Adult mouse sensory neurons on microelectrode arrays exhibit increased spontaneous and stimulus-evoked activity in the presence of interleukin-6

Bryan J. Black,[1] Rahul Atmaramani,[1] Rajeshwari Kumaraju,[1] Sarah Plagens,[1] Mario Romero-Ortega,[1] Gregory Dussor,[2] Theodore J. Price,[2] Zachary T. Campbell,[3] and Joseph J. Pancrazio[1]

[1]*Department of Bioengineering, The University of Texas at Dallas, Richardson, Texas;* [2]*School of Behavioral and Brain Sciences, The University of Texas at Dallas, Richardson, Texas; and* [3]*Department of Biological Sciences, The University of Texas at Dallas, Richardson, Richardson, Texas*

Submitted 5 March 2018; accepted in final form 10 June 2018

Black BJ, Atmaramani R, Kumaraju R, Plagens S, Romero-Ortega M, Dussor G, Price TJ, Campbell ZT, Pancrazio JJ. Adult mouse sensory neurons on microelectrode arrays exhibit increased spontaneous and stimulus-evoked activity in the presence of interleukin-6. *J Neurophysiol* 120: 1374–1385, 2018. First published June 27, 2018; doi:10.1152/jn.00158.2018.—Following inflammation or injury, sensory neurons located in the dorsal root ganglia (DRG) may exhibit increased spontaneous and/or stimulus-evoked activity, contributing to chronic pain. Current treatment options for peripherally mediated chronic pain are highly limited, driving the development of cell- or tissue-based phenotypic (function-based) screening assays for peripheral analgesic and mechanistic lead discovery. Extant assays are often limited by throughput, content, use of tumorigenic cell lines, or tissue sources from immature developmental stages (i.e., embryonic or postnatal). Here, we describe a protocol for culturing adult mouse DRG neurons on substrate-integrated multiwell microelectrode arrays (MEAs). This approach enables multiplexed measurements of spontaneous as well as stimulus-evoked extracellular action potentials from large populations of cells. The DRG cultures exhibit stable spontaneous activity from 9 to 21 days in vitro. Activity is readily evoked by known chemical and physical agonists of sensory neuron activity such as capsaicin, bradykinin, PGE_2, heat, and electrical field stimulation. Most importantly, we demonstrate that both spontaneous and stimulus-evoked activity may be potentiated by incubation with the inflammatory cytokine interleukin-6 (IL-6). Acute responsiveness to IL-6 is inhibited by treatment with a MAPK-interacting kinase 1/2 inhibitor, cercosporamide. In total, these findings suggest that adult mouse DRG neurons on multiwell MEAs are applicable to ongoing efforts to discover peripheral analgesic and their mechanisms of action.

NEW & NOTEWORTHY This work describes methodologies for culturing spontaneously active adult mouse dorsal root ganglia (DRG) sensory neurons on microelectrode arrays. We characterize spontaneous and stimulus-evoked adult DRG activity over durations consistent with pharmacological interventions. Furthermore, persistent hyperexcitability could be induced by incubation with inflammatory cytokine IL-6 and attenuated with cercosporamide, an inhibitor of the IL-6 sensitization pathway. This constitutes a more physiologically relevant, moderate-throughput in vitro model for peripheral analgesic screening as well as mechanistic lead discovery.

Address for reprint requests and other correspondence: J. J. Pancrazio, Dept. of Bioengineering, The Univ. of Texas at Dallas, 800 W. Campbell Rd., Richardson, TX 75080 (e-mail: joseph.pancrazio@utdallas.edu).

dorsal root ganglion; microelectrode arrays; nociceptors; sensitization

INTRODUCTION

The dorsal root ganglia (DRG) are collections of first-order sensory neurons involved in the perception of innocuous as well as noxious stimuli. On suprathreshold stimulation of peripheral nerve terminals, afferent fibers from the DRG are depolarized, propagating signals in the form of all-or-nothing action potentials toward the spinal cord to be processed by the central nervous system. After an injury, inflammatory cues enhance spontaneous and stimulus-evoked activity in nociceptive primary afferents (Davidson et al. 2014; Djouhri et al. 2015; Kim et al. 2016; White et al. 2005). These changes are mediated by complex signaling cascades involving myriad proinflammatory mediators such as interleukin-6 (IL-6) and nerve growth factor (NGF). Their mechanisms of action impact many cellular processes. However, our understanding of their effects on sustained neuronal activity is incomplete, owing to the technical challenge of obtaining reproducible long-term electrophysiological recordings.

Chronic pain is the most common cause of long-term disability in the world [Institute of Medicine (US) Committee on Advancing Pain Research, Care, and Education 2011], yet pharmacological treatment options for chronic pain are limited and problematic. The most prevalent approach involves prescription opioids, which are associated with high incidence of adverse effects, most prominently, addiction (Volkow and Collins 2017). Modern analgesic discovery has been largely driven by the identification of molecular targets or pathways associated with a particular pathology where modulation may then impact disease progression (Bleicher et al. 2003). However, a complementary or even alternative approach has emerged with the advent of cell- or tissue-based phenotypic screening assays. Rather than focusing on the activity of a molecular target, phenotypic (or function-based) assays capture complex cellular-level behaviors or traits that are physiologically relevant to a pathology without relying on the identification of a specific drug target or a corresponding hypothesis concerning its role in pathology.

To date, in vitro data regarding primary sensory neuron excitability and sensitization have been principally derived from single-cell patch-clamp recordings and have provided tremendous insights into the changing electrophysiological profiles of DRG neurons after exposure to inflammatory cytokines (e.g., Fischer et al. 2017; Ke et al. 2012; Wang et al. 2007). However, patch-clamp methods are invasive, incompatible with long-term measurements, and low-throughput. Substrate-integrated microelectrode arrays (MEAs), however, enable label-free, long-term measurements of action potentials from large populations of cells, potentially making them a suitable platform for function-based pharmacological and toxicological screening paradigms (Johnstone et al. 2010; Xiang et al. 2007).

Rodent DRG neurons cultured on microelectrode arrays have previously been used to study cold and heat sensitivity in the cases of both native tissue and tissue expressing gain-of-function sodium channel mutations (Pearce et al. 2005; Yang et al. 2016). However, the scope of these studies was restricted to temperature-evoked activity, and they were carried out within 1 h and 3 days of cell seeding, respectively. One previous study has reported detailed characterization of spontaneous and chemically evoked activity using embryonic rat DRG neurons on a multiwell MEA platform (Newberry et al. 2016). A limitation of this work is reliance on embryonic tissue, however. Although embryonic tissue is readily amenable to in vitro culture due to increased viability (Eide and McMurray 2005), there are significant disadvantages driven by widespread changes in gene expression that emerge later in development. These include changes linked to the voltage-gated Na channel $Na_V1.8/1.9$ (Benn et al. 2001), mRNA associated with axonal transport, vesicle trafficking, and axonal protein synthesis (Gumy et al. 2011). Additionally, dissociated embryonic and neonatal cultures of DRG neurons show little or no apparent NGF-induced sensitization to capsaicin (Zhu and Oxford 2011), unlike adult DRG in vivo and in vitro. Additionally, single-well MEAs have been used to evaluate spontaneous and evoked activity from human DRG neurons obtained from tissue donors (Enright et al. 2016). Although this approach may be ideal in terms of relevant ion channel expression and phenotype, the prospect of operating high-content, high-throughput screening with donated human tissue would be very challenging given the low anticipated cell yield (Valtcheva et al. 2016).

Here, we report a detailed study of spontaneous and evoked activity using adult murine DRG neurons cultured on substrate-integrated MEAs. Spontaneous action potentials (or spikes) emerged within 24 h of culture, reaching a peak mean spike rate at 9 days in vitro (DIV). Increased activity was reproducibly evoked by both chemical and physical agonists (capsaicin, bradykinin, temperature increase, and electrical field stimulation) by DIV 7, and spontaneous activity could be transiently decreased by relatively high-frequency electrical stimulation ($\geq$100 Hz). Most importantly, both spontaneous and evoked activity were potentiated by short- and long-term incubation with inflammatory cytokine IL-6, and persistent sensitization to capsaicin (following IL-6 washout) was induced by $\geq$24-h incubation with the cytokine. The acute effects of IL-6 were diminished in the presence of the MAPK-interacting kinase 1 inhibitor cercosporamide. In total, these findings suggest that adult DRG cultures on multiwell plates of microelectrode arrays may enable a stable, moderate-throughput, high-content platform for screening peripheral analgesics and conducting mechanistic studies pertaining to sensory neuron hyperexcitability.

MATERIALS AND METHODS

Reagents. Laminin, poly-D-lysine, polyethyleneimine, Hank's balanced salt solution (HBSS), collagenase, trypsin, glial-derived neurotrophic factor (GDNF), uridine, and 5-fluoro-2′-deoxyuridine were purchased from Sigma-Aldrich (St. Louis, MO). Fetal bovine serum (FBS), Dulbecco's modified Eagle's medium-nutrient mixture F-12 (DMEM/F-12) + GlutaMAX, and DNase were purchased from Thermo Fisher Scientific (Waltham, MA). Complete cell medium refers to DMEM/F-12 + GlutaMAX, 10% FBS, 1% penicillin-streptomycin, and 5 ng/ml GDNF.

Primary DRG extraction and culture. This study was carried out in accordance with the recommendations of the University of Texas at Dallas' Institutional Animal Care and Use Committee, which approved the protocol. Euthanasia was conducted in accordance with the American Veterinary Medical Association *Guidelines for the Euthanasia of Animals*. Adult Institute for Cancer Research (CD-1) mice (4–6 wk old; Envigo) were anesthetized with 3% isoflurane and euthanized by cervical dislocation. DRG were dissected as previously described (Sleigh et al. 2016). Briefly, the spinal column was isolated and hemisected, and the spinal cord was carefully removed to expose the DRG. DRG were individually isolated from central/peripheral roots and placed in ice-cold HBSS. DRG were transferred to dissociation solution, which consisted of collagenase (2 mg/ml) and DNase (0.1 mg/ml) and incubated for 40 min at 37°C. After 40 min, trypsin (0.025%) was added, and the solution was incubated for an additional 5 min at 37°C. The tissue was then triturated with a fire-polished glass Pasteur pipette until the solution appeared homogeneous. The solution was passed through a 70-μm nylon filter, and the volume was tripled by adding DMEM/F-12 + 10% fetal bovine serum to quench trypsinization. The cells were collected by centrifugation (10 min at 600 *g*), and the resulting pellet was resuspended in fresh complete medium. Five to ten microliters of medium containing an estimated 10,000 cells were seeded at the center of each MEA device or glass-bottomed plate. The plates were incubated at 37°C and 10% CO_2 for 30 min to allow cells to adhere, and then each well was carefully flooded with 600 μl of fresh, preheated complete medium. Cell cultures were maintained at 37°C, 10% CO_2, and 95% humidity. One hundred percent media exchanges were performed after the 1st 24 h and every alternate day afterward. After nonneuronal cells reached 90% confluence (DIV 5–7), media were supplemented with mitotic inhibitors uridine (17.5 μg/ml) and 5-fluoro-2′-deoxyuridine (7.5 μg/ml).

Multiwell microelectrode array plate preparation. DRG cells were cultured on 12-well MEA devices from Axion BioSystems (Atlanta, GA) for electrophysiological recording as well as multiwell glass-bottomed culture plates for immunocytochemical (ICC) characterization. The day before dissection, the center of each well of the MEA devices was coated with polyethyleneimine (0.1%); glass-bottom wells were coated with poly-D-lysine (50 μg/ml). Plates were incubated at 37°C and 10% CO_2 overnight. The following morning, plates were rinsed three times with sterile double-deionized water and allowed to dry. Ten microliters of laminin (20 μg/ml) was added to the center of each well and incubated at 37°C for 2 h. Laminin was removed immediately before cell seeding.

Extracellular recordings and stimulation. Extracellular voltage recordings were acquired from each multiwell plate every alternate day, beginning on *day in vitro* (DIV) *3*, using 12-well MEA plates (768 total electrodes) and the Axion Maestro multiwell plate recording system (Axion BioSystems). All baseline recordings were carried out for 30 min at 37°C and 5% CO_2. Continuous data were acquired simultaneously at 12.5 kHz per electrode and filtered using a 1-pole

Butterworth band-pass filter (200–3,000 Hz). Individual spikes were detected by filtered continuous data crossing of a 5.5-σ adaptive threshold. Unless otherwise stated, an active electrode was defined by ≥5 spikes per baseline recording session constituting a characteristic waveform (single unit). Additional analysis (e.g., mean firing rate, synchrony index) was carried out using NeuroExplorer software (Nex Technologies, Madison, AL) in combination with Axion's AxIS Metric program. To avoid unanticipated long-term changes in baseline activity due to repeated pharmacological treatments, separate cultures were designated for spontaneous and evoked recordings.

Electrical stimulation and recording was performed using Axion's Stimulation Studio in combination with software solutions provided by AxIS 2.3. Briefly, 7–8 active electrodes in each well (n = 42 electrodes) were selected and stimulated with a 100-Hz cathodic-leading biphasic square pulse train (×10 stimuli) with an amplitude of 1.2 V and pulse duration of 750 μs/phase. To determine whether the number of units stimulated were nociceptors, 10 nM, 100 nM, or 1 μM capsaicin treatment was performed after the electrical stimulation events. Unless otherwise stated, all data associated with electrical stimulations were visualized and analyzed in Axion's Neural Metric Tool software.

Pharmacological exposure. All compounds were reconstituted in DMSO, ethanol, or deionized water at ≥100× working concentrations. Preliminary experiments indicated that full bath exchange caused short-term but significant changes in baseline activity. Therefore, all pharmacological compounds were added as high-concentration, low-volume boluses to the corners of wells and mixed once with a 100-μl pipette. Before addition of compounds, a 30-min baseline recording was performed simultaneously for all experimental, vehicle, and control conditions. To establish a baseline for evoked responsiveness to chemical agonists, adult DRG at DIV 10–16 were exposed to either 100 nM bradykinin or 10 nM capsaicin for 5 min. Next, a 100% medium exchange was performed, and cells were incubated with either 1 μM prostaglandin E_2 (PGE_2) for 10 min or 100 ng/ml interleukin-6 (IL-6) for a period of 3, 24, or 48 h. To test cytokine-mediated evoked responsiveness after incubation with PGE_2 or IL-6, cells were challenged with 100 nM bradykinin or 10 nM, 100 nM, and 1 μM capsaicin, respectively. In addition, temperature increase on naïve and IL-6-treated cells was performed using the Environmental Control module in AxIS 2.3. Briefly, after a 30-min baseline recording at 37°C, the temperature was increased incrementally at ~0.5°/min to 42°C, whereas changes in activity were captured via simultaneous recordings.

Immunocytochemistry. Primary adult DRG cultures at DIV 11–13 were fixed with 4% paraformaldehyde for 10 min, washed thrice with ice-cold PBS, and permeabilized with 0.25% Triton X-100 for 30 min at room temperature (RT). Nonspecific binding sites were blocked with 10% normal goat serum (NGS) for 2 h, and primary antibodies against Neurofilament 200 (1:1,000; Sigma, St. Louis, MO), isolectin B4 (IB4; 1:1,000; Thermo Fisher Scientific), calcitonin gene-related peptide (CGRP; 1:1,000; Peninsula, San Carlos, CA) were diluted in PBS with 10% NGS and incubated overnight at 4°C. The following day, cells were incubated with species-specific secondary antibodies for 1 h at RT. Transient receptor potential vanilloid 1 (TRPV1) staining following incubation with IL-6 or naïve groups was performed using primary antibodies against TRPV1 (1:1,000; Neuromics, Edina, MN) and NeuN (1:500; Abcam, Cambridge, MA) diluted in PBS + 10% NGS and incubated for 2 h at RT. Samples were incubated with species-specific secondary antibodies for 1 h at RT. Unless stated otherwise, nuclei in all samples were visualized using 1 μg/ml 4′,6′-diamidino-2-phenylindole (Vector).

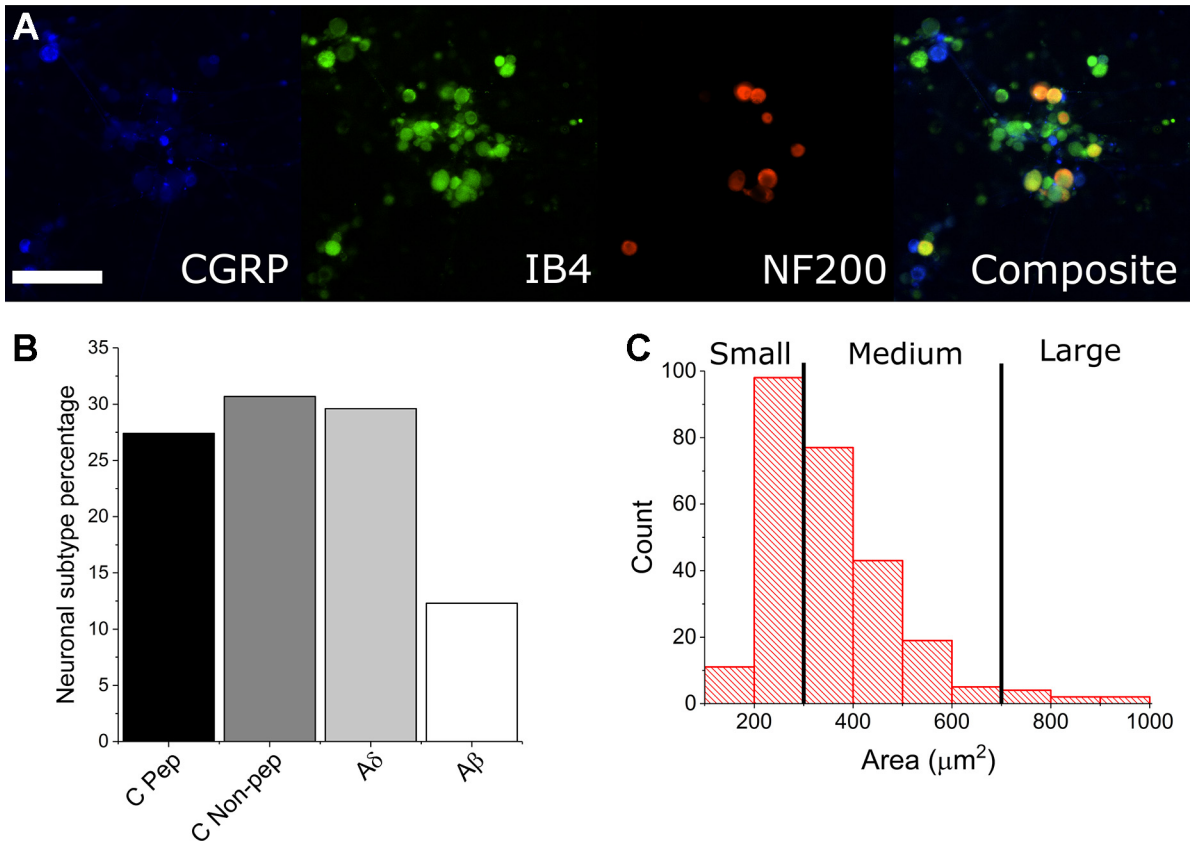

Fig. 1. Immunocytochemistry and size-based discrimination of neuronal subtypes. *A* and *B*: CGRP-positive cells (blue) indicate peptidergic C-fiber neurons (C Pep). Isolectin B4 (IB4)-positive (green), Neurofilament 200 (NF200)-negative cells indicate nonpeptidergic C-fiber neurons (C Non-pep). IB4-positive, NF200-positive (red) cells indicate Aδ-fiber neurons. NF200 (only)-positive cells indicate Aβ-fiber neurons. Scale bar represents 200 μm. *C*: automated measurements of cross-sectional area suggest a large percentage of small- and medium-gauge neurons, indicating a primarily nociceptive cell population.

Fluorescence microscopy and image analysis. All epifluorescence and confocal imaging was performed at ×20 magnification using an inverted microscope (Nikon Eclipse Ti; Nikon, Tokyo, Japan) and epifluorescent light sources (Lumencor, Beaverton, OR). To determine the percentage of distinct neuronal subtypes in the existing culture preparation, three regions of interest were acquired in separate wells ($n = 6$). To quantify the expression of TRPV1 after treatment with IL-6 or in naïve preparations, three defined regions of interest were used to visualize a minimum of 50 neuronal somata in a single field of view ($n = 3$ for treatment, $n = 3$ for naïve). All multichannel images were processed in ImageJ (NIH). Briefly, a user-defined threshold was applied to each channel, and neuronal somata were manually counted based on maximum-intensity projections. Cell counts were further analyzed, quantified, and plotted using OriginPro software (OriginLab, Northampton, MA).

Statistical analysis. To be considered for analysis, only active electrodes were chosen based on a criteria of an electrode having a mean firing rate of >1 spike/min. In the case of responsiveness to chemical agonists (bradykinin and capsaicin), an electrode qualified as responsive if the peak firing rate after treatment was at least twice that of the peak mean firing rate during baseline. All statistical analysis and data visualization was performed in OriginPro 2017 (OriginLab). Before group or pairwise tests, Shapiro-Wilk normality tests were performed. Pairwise tests were carried out using Mann-Whitney test or two-sample proportion test. In all cases, $P < 0.05$ was considered as statistically significant. Statistics are reported as $Z(n) = z$-metric, P value, type of statistical test. In cases where n numbers were unequal between treatment groups, the lower n is reported. Wellwise parameters are presented as means ± standard error of the mean (SE) unless stated otherwise.

RESULTS

Culture and population. To determine whether dissociated adult mouse DRG cultures would develop stable spontaneous activity profiles and warrant further nociceptive studies, we dissected and cultured DRG from 4- to 6-wk-old male Institute for Cancer Research (CD-1) mice onto multiwell MEAs as well as glass-bottomed dishes for morphological and ICC characterization. The presented data represent recordings from 144 microelectrode wells prepared from dissection from 24 mice. Figure 1*A* shows neuronal subtype ICC staining based on overlaps of CGRP, IB4, and NF200 expression. ICC indicated that ~95% of the cellular population by DIV 15 was nonneuronal and most likely a combination of fibroblasts, satellite glia, and Schwann cells. Of the neuronal population, ~88% were found to be either CGRP- or IB4-positive (nociceptive). Furthermore, we have measured the cross-sectional area of neuronal cell types and found ~97% to be of the small or medium gauge, based on previous size-based characterizations of DRG cell subtypes (Newton et al. 2001). These data suggest that we have cultured a largely nociceptive neuronal population and indicate that we were able to culture with sufficient density and viability for long-term MEA recordings.

Spontaneous activity. After a single DIV, action potentials could be readily recorded with excellent signal-to-noise ratios [12.3 (6.8), $n = 64$, mean (SD)] and manually sorted into single units based on characteristic waveform shapes (Fig. 2, *B* and *C*). Individual recording sites on microelectrode arrays in contact with neural tissue, both in vivo and in vitro, often detect >1 unit or distinct bioelectrical signal source. To determine whether our analysis of individual recording channels would reflect single cells (single units), waveforms were sorted in 12 representative wells on DIV 15. Only 29 out of 384 active

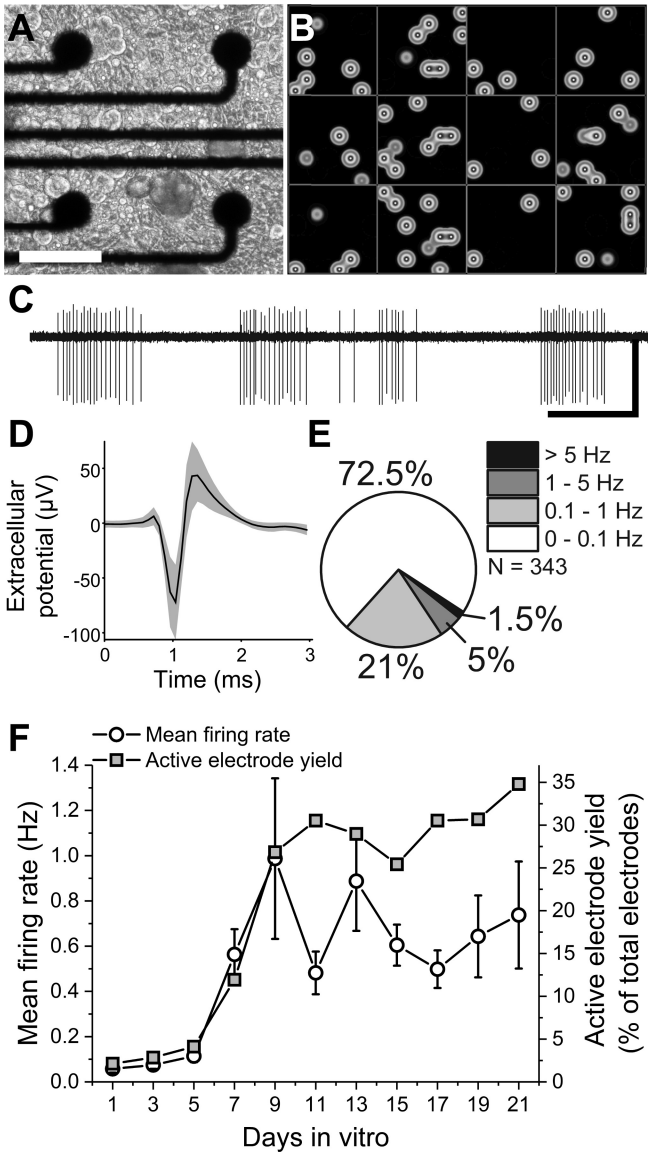

Fig. 2. Dorsal root ganglia (DRG) neurons exhibit well-resolved, stable spontaneous activity in vitro. *A*: phase image of disorganized dissociated DRG neuron culture. Scale bar represents 100 μm. *B*: heat map of 12-well multiwell microelectrode array recording. Each box indicates a single well. Each spot indicates electrode activity integrated over a 1-s period. *C*: representative trace of filtered continuous recording from a single electrode. Scale bars represent 1 s (horizontal) and 75 μV (vertical). *D*: representative mean waveform ± SD for a single unit. *E*: percentages of spontaneously active channels in terms of spontaneous firing rates. *F*: mean firing rate and active electrode yield over 21 days in vitro.

channels exhibited >1 unit (7.6%), indicating that under our culture conditions the recordings from individual microelectrode sites likely correspond to a single bioelectric source. Therefore, all additional analyses were carried out with the assumption that channel recordings represented single cells. Whereas the signal-to-noise ratio did not significantly change over time, the spontaneously active electrode yield increased from 2.1 to 26% between DIV 1 and 9 [$Z(768) = 5.4$, $P = 7.9\text{E}{-8}$, 2-sample proportion test]. Over the same duration, the mean firing rate per well increased from 0.05 ± 0.01 to 0.99 ± 0.35 Hz [$Z(12) = 3.8$, $P = 1.4\text{E}{-4}$, Mann-Whitney test]. However, neither the mean firing rate nor the active

electrode yield changed significantly between DIV 9 and 21 [Fig. 2*F*; $\chi^2(12) = 0.79$, $P = 0.38$, Kruskal-Wallis ANOVA], suggesting the establishment of a stable baseline activity over time courses sufficient for pharmacological studies. The observed mean firing rates were relatively low compared with those reported in studies of cortical (Charkhkar et al. 2014) and ventral horn motor neurons (Black et al. 2017), but not embryonic DRG cultures (1.14 ± 0.12 Hz, Newberry et al. 2016), and were significantly skewed toward lower firing rates. Of the recorded units, 72.5% were found to have firing rates ≤0.1 Hz, whereas only 1.5% of units had firing rates of >5 Hz (Fig. 2*E*). Importantly, however, this range of spontaneous firing rates is consistent with previously reported spontaneous firing of nociceptors from the lumbar vertebrae L4/L5 DRG in vivo, where observations have ranged between 0.01 and 1.3 Hz (Djouhri et al. 2006), with a high percentage of neurons exhibiting little to no spontaneous activity (range: 4.8–6.8%; Liu et al. 2000). The relatively minor reduced firing rate and skewness in our distribution compared with embryonic DRG recordings may be attributed to methodological differences in analysis, including active channel criterion, or to intrinsic firing rate differences due to tissue derivation at different stages of cellular maturity (National Research Council 2009).

Additionally, we observed distinct differences in the firing patterns across recording channels. Figure 3 shows representative raster plots and interspike interval (ISI) histograms of four spontaneously active electrodes from a single well. Overall, the ISI coefficient of variation (CV) was 1.62 ± 0.03 for spontaneous activity on DIV 12. This is in contrast to reported CVs for embryonic cultures (0.91 ± 0.05, DIV 14) and suggests a higher incidence of intrinsic bursting (Stiefel et al. 2013; Svirskis and Rinzel 2000) in adult cultures. However, we observed only 1.3% of active electrodes exhibiting synchronous or correlated activity. To determine whether these correlated electrode recordings were a single neuron extending processes across multiple electrodes or were representative of functional connections, we treated wells in which correlated activity was observed with either synaptic vesicle blocker botulinum neurotoxin A (100 ng/ml, 24-h incubation) or gap junction inhibitor carbenoxolone (50 μM, 10-min incubation). In only 3 cases (out of 10) did we observe any reduction in correlation or firing rates following treatment with carbenoxolone (0 out of 3 in the case of botulinum neurotoxin A), suggesting that the few functional connections that exist may be mediated by gap junctions but not by synaptic transmission.

Evoked activity. To determine whether adult DRG cultures were sensitive to known chemical and physical agonists of sensory neuron activity, they were treated with 10 nM capsaicin, 100 nM bradykinin, or 1 μM prostaglandin E_2 (PGE_2) or were subject to increased temperature or electrical field stimulation.

Capsaicin responsiveness. Figure 4*A* shows representative raster plots from six electrodes responsive to 10 nM capsaicin within a single well. In total, 27% of previously active channels responded to 10 nM capsaicin, and the wellwise mean firing rate was found to increase from 1.1 ± 0.2 to 2.6 ± 0.5 Hz [$Z(101) = 4.84$, $P = 1.3\text{E}{-6}$, Mann-Whitney test]. Both the percentage of responsive electrodes and the evoked mean firing rates were found to increase with increased capsaicin concentration. 27, 36.6, And 39.1% of electrodes were found to be responsive to 10, 100, and 1,000 nM capsaicin, respectively [$Z(101) = 6.4$, $P = 1.9\text{E}{-10}$ for 1,000 nM, 2-sample proportion test]. These values are highly consistent with previous reports of colocalization of neuronal markers in the DRG, including TRPV1 (Price and Flores 2007), but are on the lower end of previously reported values of capsaicin responsiveness in vitro (Gold et al. 1996; Malsch et al. 2014; Tsantoulas et al. 2013). These differences are likely attributable to approaches in cell culture (embryonic vs. adult, lumbar only vs. lumbar and cervical DRG), methodology (calcium imaging vs. patch-clamp vs. MEA), and/or definition of responsiveness.

Temperature sensitivity (42°C). Following baseline recordings, calibrated temperature increases were induced via the stage plate heater of the recording system. Approximately 38.9% of channels were responsive at 42°C or during the temperature rise. Overall normalized mean firing rates were observed to increase significantly, reaching a steady, elevated state after reaching 42°C (Fig. 4*B*), and returned to baseline levels following stage plate cooling. These data suggest that calibrated stage plate heating may be used as a measure of

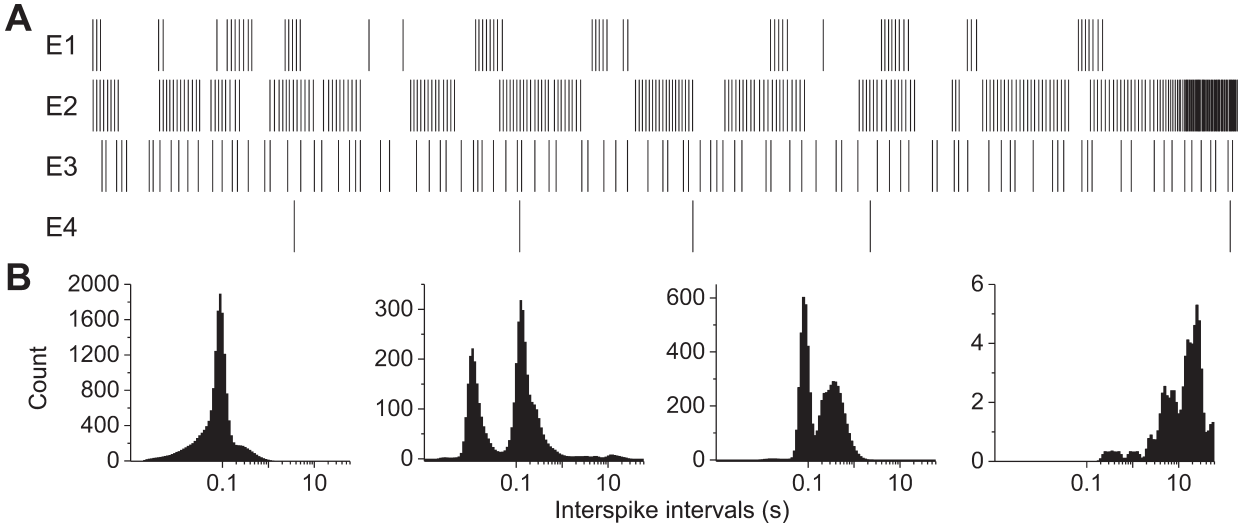

Fig. 3. Spontaneously active DRG neurons exhibit various firing patterns in vitro. *A*: representative raster plots from 4 spontaneously active electrodes (E) within a single well exhibiting different firing patterns. *B*: associated interspike interval histograms.

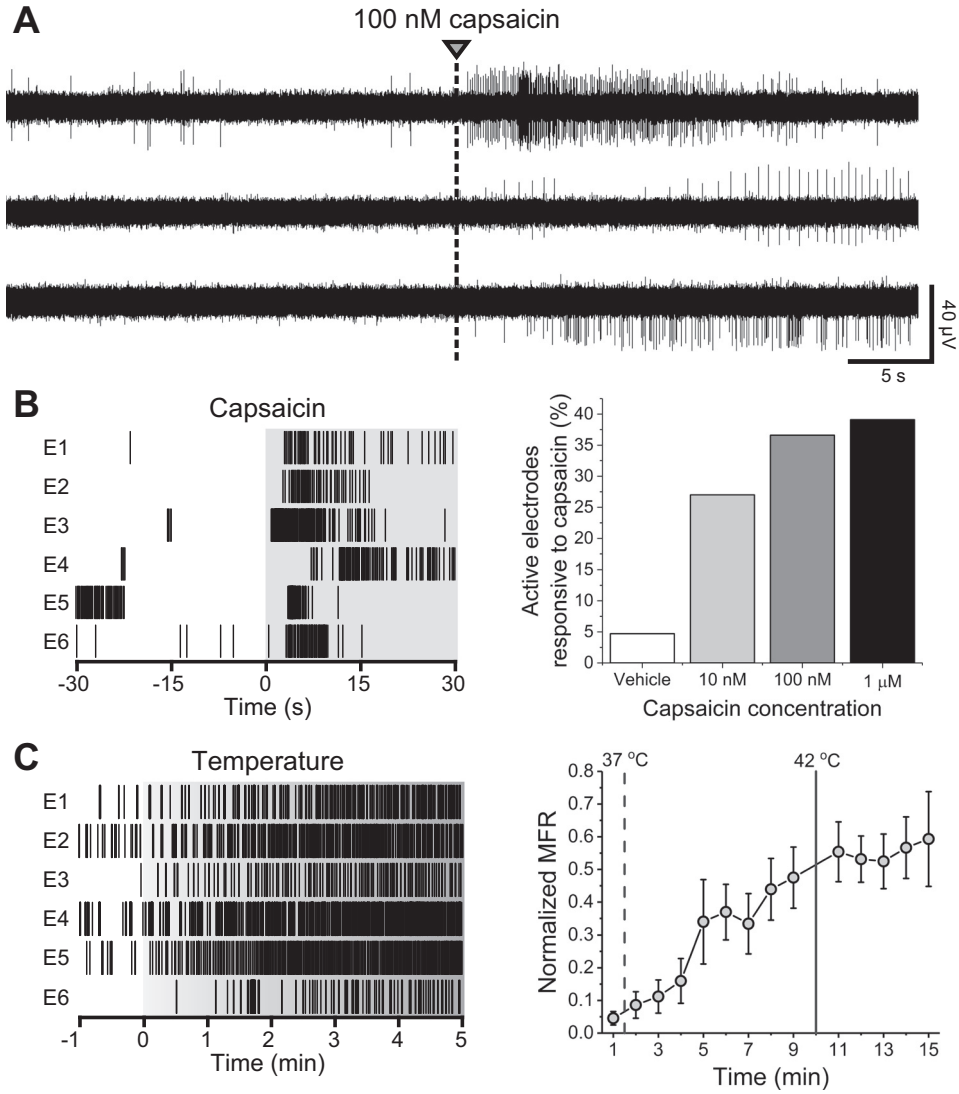

Fig. 4. Capsaicin and temperature responsiveness. *A*: representative continuous data traces from electrodes within a single well exhibiting responsiveness to 100 nM capsaicin. *B*: representative raster plots from 6 10 nM capsaicin-responsive electrodes (E) within a single well (*left*) and capsaicin concentration responsiveness as a percentage of active electrodes (*right*). *C*: representative raster plots from 6 temperature-responsive electrodes within a single well (*left*). Normalized mean firing rate (MFR) during calibrated temperature increase from 37 to 42°C.

sensitivity for adult DRG neurons in vitro and, interestingly, that functional temperature sensitivity of these cultures lies well below levels typically defined as noxious (42°C). This is likely due, although not investigated here, to conserved expression of cation channels with sensitivity at or below 40°C, such as TRPV4, which is expressed in rodent DRG in vitro as well as in vivo (Cao et al. 2009; Chen et al. 2007; Suzuki et al. 2003; Veldhuis and Bunnett 2013; Wang et al. 2015).

Bradykinin and PGE_2 responsiveness. Treatment with either 100 nM bradykinin or 1 μM PGE_2 resulted in significant increase in mean firing rate on 43 and 35% of previously active channels, respectively. In contrast to capsaicin, the onset of bradykinin- and PGE_2-evoked activity was relatively slow, reaching its mean peak at 60 and 70 s, respectively (30-s bins), whereas capsaicin-evoked activity reached its mean peak within 10 s (Fig. 5). Moreover, the time required for return to baseline was also increased, requiring ~2 min in the case of bradykinin and >12 min in the case of PGE_2. In comparison, capsaicin-treated wells returned to baseline or exhibited reduced activity within 40 s.

Electrical field stimulation. Electrical field stimulation was carried out using recording electrodes with previously observed spontaneous activity. Single biphasic pulses were found to be ineffective at eliciting activity within the range of amplitude/duration parameters available through the Axion Maestro system. However, we observed differential responsiveness (both activation and inhibition) on a large subset of stimulated microelectrodes (83.3%) in response to pulse trains of 10 cathodic-leading biphasic square pulses (1.2 V, 750-μs phase duration) at or above 100 Hz. 54.8% Exhibited activation only (evoked activity), 11.9% exhibited inhibition only (reduced activity compared with baseline), and 16.7% exhibited activation followed by inhibition (Fig. 6, *A* and *B*). For stimulated channels exhibiting inhibition, the mean time to return to baseline was 19.2 ± 2.8 s. For stimulated channels exhibiting activation, the mean time to return to baseline was 3.0 ± 0.4 s.

To determine whether activation or inhibition outcomes were associated with nociceptive cell types, we followed electrical stimulation experiments with 1 μM capsaicin treatment. Figure 6*C* shows the percentage of electrodes exhibiting different responses to electrical stimulation that were also responsive to capsaicin. Although the relative *n* number of capsaicin-responsive electrodes was low (between 3 and 8), these data suggest that differential responsiveness to electrical stimulation is not indicative of neuronal subtype.

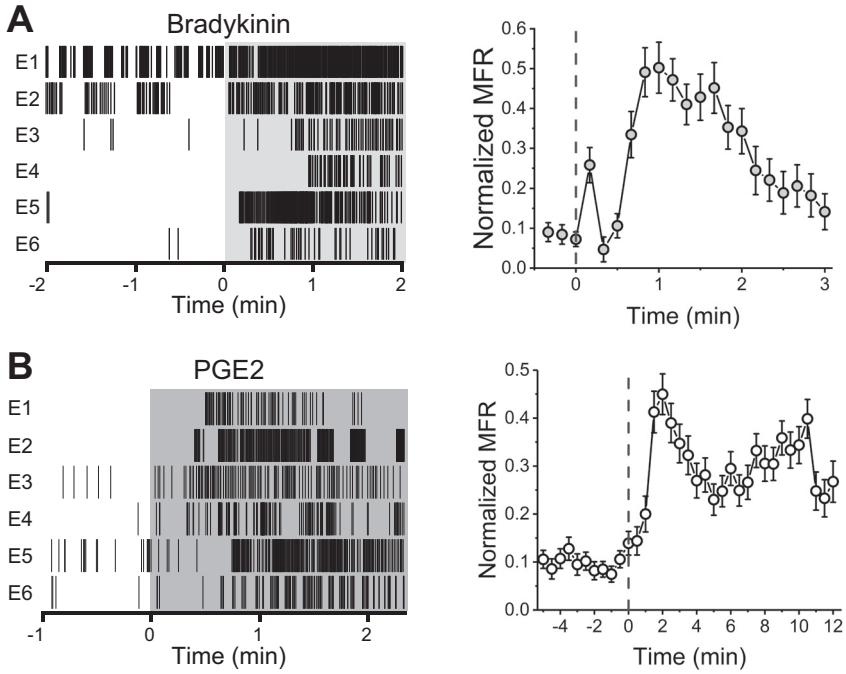

Fig. 5. Bradykinin and PGE_2 responsiveness. *A*: representative raster plots from 6 10 nM bradykinin-responsive electrodes (E) within a single well (*left*) and normalized mean firing rates (MFR) before and after bradykinin addition (*right*). *B*: representative raster plots from 6 PGE_2-responsive electrodes within a single well (*left*) and normalized mean firing rate before and after addition of PGE_2.

Short- and long-term excitability changes in the presence of IL-6. To determine whether primary adult DRG culture activity could be potentiated by inflammatory cytokines, recordings were carried out in the absence and presence of 100 ng/ml IL-6 at 0- and 48-h time points relative to IL-6 addition. Thirty-minute baseline recordings were followed by either 3-h or 30-min continuous recordings in the presence of IL-6 or vehicle (water). Figure 7*A* shows short-term (0–3 h) responsiveness to IL-6, which was observed on 41% of previously active channels. Overall, median firing rates significantly increased from 0.02 to 0.15 Hz over the 3 h of IL-6 exposure [$Z(203) = 10.4$, $P = 3.5\text{E}{-25}$, Mann-Whitney test]. Additionally, median ISI CVs also significantly increased from 1.13 to 2.29 in the presence of IL-6 [$Z(203) = 12.3$, $P = 1.6\text{E}{-34}$], suggesting an increase in intrinsic bursting behavior. However, no significant differences were observed in terms of mean spike amplitude [40.6 ± 5.3 vs. 43.5 ± 2.7 μV; $Z(203) = 0.17$, $P = 0.87$, Mann-Whitney test]. After 48-h incubation, IL-6-treated cultures still exhibited both increased spontaneous firing rates [$Z(203) = 4.8$, $P = 1.52\text{E}{-6}$, Mann-Whitney test] and increased ISI CVs [$Z(103) = 3.0$, $P = 0.002$, Mann-Whitney test] compared with baseline, suggesting long-term hyperactivity in the presence of IL-6 (Fig. 7*B*).

Previous work from our group (Moy et al. 2017) demonstrated reduced short-term responsiveness to IL-6 in cultures prepared from mice lacking eukaryotic translation initiation factor 4E phosphorylation. To determine whether IL-6-induced hyperexcitability could be reduced by eukaryotic translation initiation factor 4E phosphorylation inhibitors, adult DRG cultures were exposed to a 30-min pretreatment with either 100 nM cercosporamide (a potent Mnk and JAK3 pathway inhibitor) or medium and equal volumes of vehicle (water) 30 min before treatment with IL-6. Vehicle-pretreated wells exhibited significant increases in spontaneous median firing rate following IL-6 exposure [$Z(37) = 2.14$, $P = 0.03$, Mann-Whitney test], whereas those pretreated with cercosporamide exhibited a significant decrease in median firing rate [$Z(80) = 0.6.1$, $P = 1.4\text{E}{-9}$, Mann-Whitney test; Fig. 7*C*]. However, there were no significant differences in terms of ISI CVs. Moreover, there was no significant difference in either median firing rate or ISI CV following 48-h incubation with IL-6.

To determine whether capsaicin-evoked activity may be potentiated by IL-6 incubation, cultures were exposed to a low concentration (10 nM) of capsaicin before and after IL-6 incubation. The number of electrodes that were responsive to 10 nM capsaicin significantly increased [$Z(69) = 2.8$, $P = 4.8\text{E}{-3}$, 2-sample proportion test] after 48-h IL-6 incubation (from 23 to 38) but not in the case of vehicle (19 to 17). Additionally, we tested 3 periods of IL-6 incubation and washout (3, 24, and 48 h), all followed by 10 nM capsaicin treatment. We found that both 24- and 48-h incubation with IL-6 were sufficient to cause increased capsaicin responsiveness but not 3-h incubation (Fig. 8*A*). These data suggest that there is a minimum incubation time necessary to elicit persistent changes in hypersensitivity to chemical stimuli in vitro.

To determine whether temperature-evoked activity may be potentiated by IL-6 incubation, adult DRG cultures were exposed to 42°C following 48-h incubation with IL-6. Temperature responsiveness was increased following 48-h IL-6 incubation. Sixty-four percent of baseline active electrodes were found to respond to temperature increase (42°C) in wells treated with IL-6, whereas only 38.9% of channels in untreated wells were found to be responsive to the same temperature increase [$Z(299) = 3.65$, $P = 2.6\text{E}{-4}$, 2-sample proportion test; Fig. 8*B*]. Temperature variations did not appear to cause significant shifts in rise time or peak firing rate between treatment groups.

To determine whether increased capsaicin and temperature responsiveness was related to expression of TRPV1, targeted ICC was carried out following 48-h incubation in either 100 ng/ml IL-6 or vehicle. Figure 8*C* shows representative labeling for TRPV1 and NeuN expression in neurons treated with IL-6.

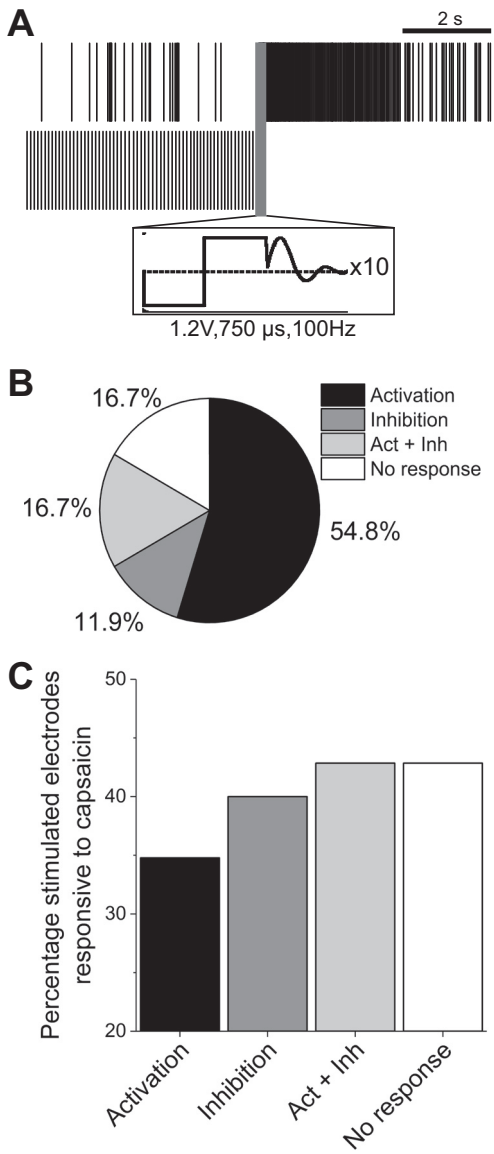

Fig. 6. Electrical stimulation at frequencies >100 Hz elicits differential responsiveness. *A*: representative raster plots from 2 stimulated electrodes exhibiting either activation (*top*) or inhibition (*bottom*) of activity. Scale bar represents 2 s. *Inset* (black square) illustrates cathodic-leading biphasic waveform and artifact removal. *B*: percentage breakdown of electrodes that were activated, inhibited, both (Act + Inh), or neither ($n = 42$). *C*: percentage of stimulated electrodes found responsive to 1 μM capsaicin.

We found a significant increase of TRPV1-positive cells following IL-6 incubation [$Z(488) = 6.0$, $P = 2.7E{-}9$, 2-sample proportion test; Fig. 8*D*].

In total, these data suggest that short- and/or long-term incubation with inflammatory cytokine IL-6 induces persistent changes in both spontaneous and stimulus-evoked activity in adult DRG cultures in vitro. Additionally, these changes in stimulus-evoked activity may be due to increased membrane expression of TRPV1.

DISCUSSION

We have carried out the first detailed characterization of spontaneous and stimulus-evoked recordings from adult mouse DRG neurons in vitro using a multiwell MEA platform for ≤21 days. Importantly, we have demonstrated differential excitability, both in terms of spontaneous firing rates/patterns and responsiveness to external stimuli, in the presence and absence of the inflammatory mediator, IL-6. IL-6 was chosen as previous studies have demonstrated both short- and long-term effects of IL-6 incubation on cultured DRG neurons (Andratsch et al. 2009; Ebbinghaus et al. 2015; Melemedjian et al. 2010; Obreja et al. 2005), and targeting IL-6 or its receptor may lead to the discovery of novel therapeutic interventions targeting pathological pain states (Zhou et al. 2016). It is worth mentioning that the model presented here does not preclude the study of other inflammatory mediators known to alter excit-

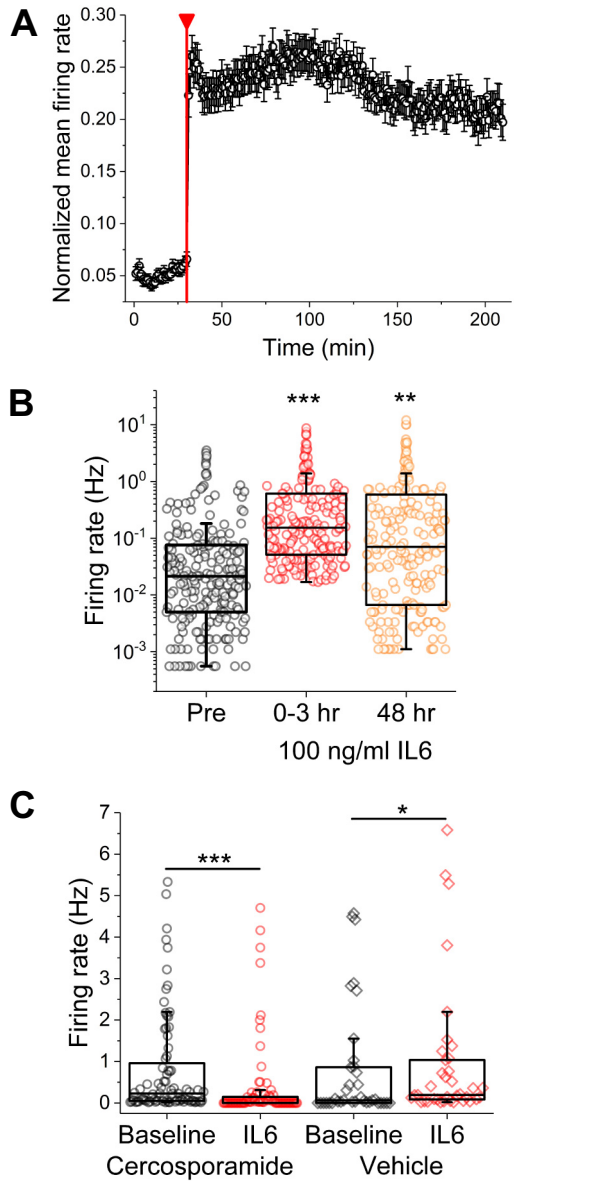

Fig. 7. Spontaneous sensory neuron activity is significantly increased with short- and long-term incubation with IL-6. *A*: normalized mean firing rate for electrode subset found to be responsive to IL-6 (41% of previously active electrodes). Red line indicates addition of 100 ng/ml IL-6. *B*: firing rates before (Pre), immediately following (0–3 h), and 48 h following IL-6 addition. Symbols represent data from single electrodes. *C*: firing rates before and immediately following IL-6 addition in the presence of vehicle (water) or MAPK-interacting kinase 1/2 inhibitor cercosporamide. $*P < 0.05$, $**P < 0.01$, and $***P < 0.001$.

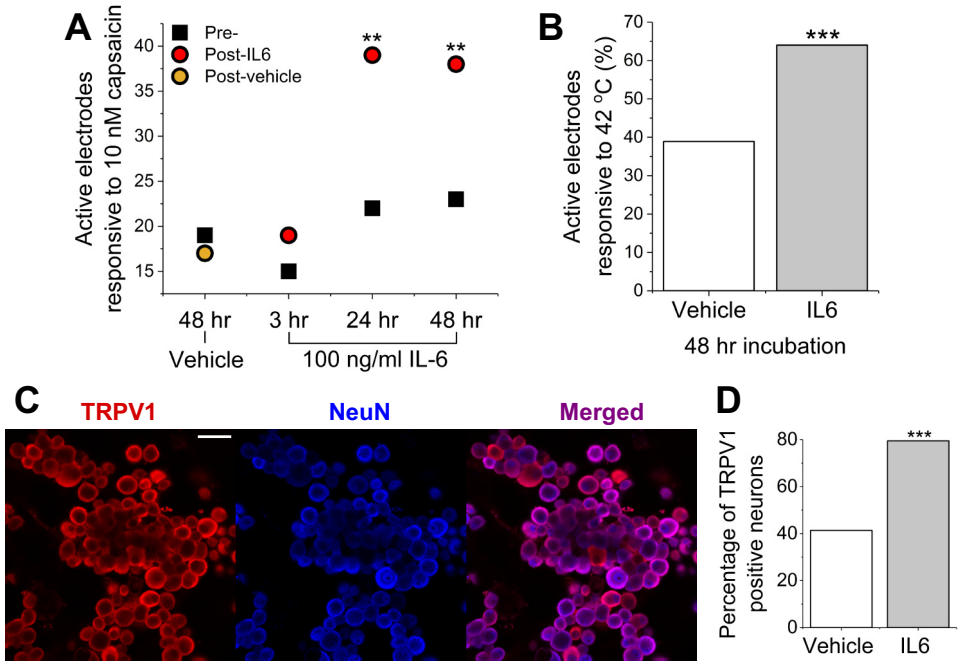

Fig. 8. Incubation with IL-6 causes increased capsaicin and temperature responsiveness. *A*: active electrodes responsive to capsaicin before treatment (Pre-) and following 3-, 24-, or 48-h incubation with IL-6 or vehicle. All treatment recordings (Post-) were carried out 48 h after baseline. *B*: active electrodes responsive to 42°C following 48-h incubation with IL-6 or vehicle. *C*: representative fluorescence images of immunocytochemistry staining for capsaicin- and temperature-sensitive cation channel transient receptor potential vanilloid 1 (TRPV1; *left*; red) and neuronal marker NeuN (blue; *middle*). Scale bar represents 100 μm. *D*: percentage of TRPV1-positive neurons following 48-h incubation with IL-6 or vehicle. $^{**}P < 0.01$ and $^{***}P < 0.001$.

ability in vivo or in vitro nor does it preclude the use of other tissue sources, including primary DRG from previously injured animals. DRG extracted from animals subjected to chronic constriction (Study and Kral 1996), thoracic spinal injury (Bedi et al. 2010), and chemotherapy-induced neuropathy have been shown to retain their hyperexcitable phenotype in vitro (Li et al. 2018).

Previous studies have reported little to no spontaneous activity from adult murine DRG neurons cultivated from uninjured animals for MEA or patch-clamp recordings (Kayano et al. 2013; Kitamura et al. 2005; Newberry et al. 2016) without the addition of relatively high concentrations of nerve growth factor (NGF). First, this highlights the ability of MEAs to capture sporadic or low-frequency spontaneous activity over time courses incompatible with whole cell patch-clamp recordings. Second, we have developed our adult DRG culture protocols specifically for MEA recording. Previously published protocols, which were developed for patch-clamp electrophysiology, called for the addition of mitotic inhibitors on seeding to limit the proliferation of nonneuronal support cells. Support cells, including satellite glial and Schwann cells, have been previously shown to promote long-term adhesion as well as increased intrinsic activity and functional connections in mixed cultures of both spinal motor neurons (Ullian et al. 2004) and retinal ganglion cells (Pfrieger and Barres 1997). Therefore, we have added relatively low concentrations of mitotic inhibitor (8.75 ng/ml uridine, 3.75 ng/ml 5-fluoro-2′-deoxyuridine) only after 5–7 days in culture, when we observed a confluent population of nonneuronal support cells. However, the extent to which specific cell culture conditions, including the presence of satellite glia and Schwann cells, may alter the spontaneously active phenotype in our preparation has not been fully explored. Although fetal bovine serum is widely used in sensory neuron culture medium preparations, lot-to-lot variation in protein and insulin concentrations may affect neuronal as well as nonneuronal phenotypes. Both satellite glial cells and Schwann cells are known to secrete NGF and GDNF in vitro and in vivo, which regulate gene expression and may also directly sensitize nociceptors (Ohara et al. 2009; Scholz and Woolf 2007; Watkins and Maier 2002). Additionally, previous studies have shown that GDNF restores expression of mRNA associated with TTX-resistant $Na_V1.9$ sodium channels following axotomy to near-normal levels as well as increases peak amplitudes of TTX-resistant currents (Fjell et al. 1999; Waxman et al. 1999). Further studies need to be undertaken to understand better the phenotypic contributions of nonneuronal cells as well as culture conditions. However, it is worth reiterating that the cultures described here demonstrated stable baseline activity that was readily increased and sensitized by application of IL-6. With the ability to monitor nociceptor activity on MEAs consistently, our work provides a potential means to dissect the contribution of individual cell types within this complex milieu of support cells to nociceptor activity. This issue is particularly attractive given the recent resurgence of interest in intercellular communication in relation to the neuroimmune interface.

We demonstrate the use of the MEA platform for pharmacological studies and extend this work to evaluate safe and effective electrical stimulation parameters in vitro. Electrical stimulation of DRG or whole nerve has found preclinical and clinical applications for transient antinociceptive effects (Kent et al. 2018). Although we were unable to match total charge delivery parameters previously reported for randomized human clinical trials (915.4 μA at 20 Hz; Deer et al. 2017) without potentially damaging the electrodes and/or tissue, we were able to deliver stimulation frequencies ($\geq$100 Hz) previously demonstrated effective for antinociceptive applications in transcutaneous electrical nerve stimulation (Hsiao et al. 2017) as well as spinal cord stimulation (Miller et al. 2016). At these frequencies, we observed distinct classes of responsiveness (activation, inhibition, and combinations thereof), none of which was found to coincide exclusively with nociceptor subtype (based on capsaicin responsive-

ness). This outcome may be attributable to the stimulated organelle and the location and orientation of the stimulating electrode relative to the stimulated organelle. As previously mentioned, our observations of morphological culture development and increasing active electrode yield suggest that we are interfacing with a combination of somata and axons. Previous studies report varying stimulation thresholds for somatic vs. axonal activation and, more importantly, that somatic membrane potentials may become increasingly depolarized compared with axons during subthreshold stimulation without generating action potentials (Radivojevic et al. 2016). Differential outcomes, in terms of activation or inhibition have also been observed at or above 100 Hz in thalamus and subthalamic neurons (Kiss et al. 2002), although the underlying mechanism is not fully elucidated. In total, this further argues for the development of compartmentalized cultures, wherein the soma and axonal processes may be electrically accessed separately. Previous studies have used compartmentalized cultures to interrogate somata vs. axons/dendrites optically, electrically, and chemically (Tsantoulas et al. 2013). A similar system may be used to test stimulation parameters on axons vs. somata to optimize efficiency and safety of electrical modulation devices further.

In summary, we have characterized a spontaneously active in vitro adult mouse DRG model using substrate-integrated multiwell MEAs. We have demonstrated stable, long-term spontaneous activity and have generated a pharmacological profile consistent with a nociceptor-rich culture that is sensitized by inflammatory mediators known to play a role in chronic pain development. In total, these finding suggest that adult mouse DRG on MEAs may serve as a potential model for peripheral analgesic and mechanistic lead discovery.

GRANTS

Z. T. Campbell was supported by National Institute of Neurological Disorders and Stroke Grant 5-R01-NS-100788-02.

DISCLOSURES

No conflicts of interest, financial or otherwise, are declared by the authors.

AUTHOR CONTRIBUTIONS

B.J.B., M.R.-O., G.D., T.J.P., Z.T.C., and J.J.P. conceived and designed research; B.J.B., R.A., R.K., and S.P. performed experiments; B.J.B., R.A., and S.P. analyzed data; B.J.B. interpreted results of experiments; B.J.B. prepared figures; B.J.B., R.A., and S.P. drafted manuscript; B.J.B., M.R.-O., G.D., T.J.P., Z.T.C., and J.J.P. edited and revised manuscript; B.J.B., R.A., R.K., S.P., M.R.-O., G.D., T.J.P., Z.T.C., and J.J.P. approved final version of manuscript.

REFERENCES

Andratsch M, Mair N, Constantin CE, Scherbakov N, Benetti C, Quarta S, Vogl C, Sailer CA, Uceyler N, Brockhaus J, Martini R, Sommer C, Zeilhofer HU, Müller W, Kuner R, Davis JB, Rose-John S, Kress M. A key role for gp130 expressed on peripheral sensory nerves in pathological pain. *J Neurosci* 29: 13473–13483, 2009. doi:10.1523/JNEUROSCI.1822-09.2009.

Bedi SS, Yang Q, Crook RJ, Du J, Wu Z, Fishman HM, Grill RJ, Carlton SM, Walters ET. Chronic spontaneous activity generated in the somata of primary nociceptors is associated with pain-related behavior after spinal cord injury. *J Neurosci* 30: 14870–14882, 2010. doi:10.1523/JNEUROSCI.2428-10.2010.

Benn SC, Costigan M, Tate S, Fitzgerald M, Woolf CJ. Developmental expression of the TTX-resistant voltage-gated sodium channels $Na_v1.8$ (SNS) and $Na_v1.9$ (SNS2) in primary sensory neurons. *J Neurosci* 21: 6077–6085, 2001. doi:10.1523/JNEUROSCI.21-16-06077.2001.

Black BJ, Atmaramani R, Pancrazio JJ. Spontaneous and evoked activity from murine ventral horn cultures on microelectrode arrays. *Front Cell Neurosci* 11: 304, 2017. doi:10.3389/fncel.2017.00304.

Bleicher KH, Böhm HJ, Müller K, Alanine AI. Hit and lead generation: beyond high-throughput screening. *Nat Rev Drug Discov* 2: 369–378, 2003. doi:10.1038/nrd1086.

Cao DS, Yu SQ, Premkumar LS. Modulation of transient receptor potential vanilloid 4-mediated membrane currents and synaptic transmission by protein kinase C. *Mol Pain* 5: 1744-8069-5-5, 2009. doi:10.1186/1744-8069-5-5.

Charkhkar H, Frewin C, Nezafati M, Knaack GL, Peixoto N, Saddow SE, Pancrazio JJ. Use of cortical neuronal networks for in vitro material biocompatibility testing. *Biosens Bioelectron* 53: 316–323, 2014. doi:10.1016/j.bios.2013.10.002.

Chen X, Alessandri-Haber N, Levine JD. Marked attenuation of inflammatory mediator-induced C-fiber sensitization for mechanical and hypotonic stimuli in $TRPV4^{-/-}$ mice. *Mol Pain* 3: 1744-8069-3-31, 2007. doi:10.1186/1744-8069-3-31.

Davidson S, Copits BA, Zhang J, Page G, Ghetti A, Gereau RW 4th. Human sensory neurons: membrane properties and sensitization by inflammatory mediators. *Pain* 155: 1861–1870, 2014. doi:10.1016/j.pain.2014.06.017.

Deer TR, Levy RM, Kramer J, Poree L, Amirdelfan K, Grigsby E, Staats P, Burton AW, Burgher AH, Obray J, Scowcroft J, Golovac S, Kapural L, Paicius R, Kim C, Pope J, Yearwood T, Samuel S, McRoberts WP, Cassim H, Netherton M, Miller N, Schaufele M, Tavel E, Davis T, Davis K, Johnson L, Mekhail N. Dorsal root ganglion stimulation yielded higher treatment success rate for complex regional pain syndrome and causalgia at 3 and 12 months: a randomized comparative trial. *Pain* 158: 669–681, 2017. doi:10.1097/j.pain.0000000000000814.

Djouhri L, Al Otaibi M, Kahlat K, Smith T, Sathish J, Weng X. Persistent hindlimb inflammation induces changes in activation properties of hyperpolarization-activated current (I_h) in rat C-fiber nociceptors *in vivo*. *Neuroscience* 301: 121–133, 2015. doi:10.1016/j.neuroscience.2015.05.074.

Djouhri L, Koutsikou S, Fang X, McMullan S, Lawson SN. Spontaneous pain, both neuropathic and inflammatory, is related to frequency of spontaneous firing in intact C-fiber nociceptors. *J Neurosci* 26: 1281–1292, 2006. doi:10.1523/JNEUROSCI.3388-05.2006.

Ebbinghaus M, Segond von Banchet G, Massier J, Gajda M, Bräuer R, Kress M, Schaible HG. Interleukin-6-dependent influence of nociceptive sensory neurons on antigen-induced arthritis. *Arthritis Res Ther* 17: 334, 2015. doi:10.1186/s13075-015-0858-0.

Eide L, McMurray CT. Culture of adult mouse neurons. *Biotechniques* 38: 99–104, 2005. doi:10.2144/05381RR02.

Enright HA, Felix SH, Fischer NO, Mukerjee EV, Soscia D, Mcnerney M, Kulp K, Zhang J, Page G, Miller P, Ghetti A, Wheeler EK, Pannu S. Long-term non-invasive interrogation of human dorsal root ganglion neuronal cultures on an integrated microfluidic multielectrode array platform. *Analyst (Lond)* 141: 5346–5357, 2016. doi:10.1039/C5AN01728A.

Fischer BD, Ho C, Kuzin I, Bottaro A, O'Leary ME. Chronic exposure to tumor necrosis factor in vivo induces hyperalgesia, upregulates sodium channel gene expression and alters the cellular electrophysiology of dorsal root ganglion neurons. *Neurosci Lett* 653: 195–201, 2017. doi:10.1016/j.neulet.2017.05.004.

Fjell J, Cummins TR, Dib-Hajj SD, Fried K, Black JA, Waxman SG. Differential role of GDNF and NGF in the maintenance of two TTX-resistant sodium channels in adult DRG neurons. *Brain Res Mol Brain Res* 67: 267–282, 1999. doi:10.1016/S0169-328X(99)00070-4.

Gold MS, Reichling DB, Shuster MJ, Levine JD. Hyperalgesic agents increase a tetrodotoxin-resistant Na^+ current in nociceptors. *Proc Natl Acad Sci USA* 93: 1108–1112, 1996. doi:10.1073/pnas.93.3.1108.

Gumy LF, Yeo GS, Tung YC, Zivraj KH, Willis D, Coppola G, Lam BY, Twiss JL, Holt CE, Fawcett JW. Transcriptome analysis of embryonic and adult sensory axons reveals changes in mRNA repertoire localization. *RNA* 17: 85–98, 2011. doi:10.1261/rna.2386111.

Hsiao HT, Chien HJ, Lin YC, Liu YC. Transcutaneous electrical nerve stimulator of 5000 Hz frequency provides better analgesia than that of 100

Hz frequency in mice muscle pain model. *Kaohsiung J Med Sci* 33: 165–170, 2017. doi:10.1016/j.kjms.2017.01.009.

Institute of Medicine (US) Committee on Advancing Pain Research, Care, and Education. *Relieving Pain in America: A Blueprint for Transforming Prevention, Care, Education, and Research*. Washington, DC: Nat. Acad. Press, 2011. doi:10.17226/13172.

Johnstone AF, Gross GW, Weiss DG, Schroeder OH, Gramowski A, Shafer TJ. Microelectrode arrays: a physiologically based neurotoxicity testing platform for the 21st century. *Neurotoxicology* 31: 331–350, 2010. doi:10.1016/j.neuro.2010.04.001.

Kayano T, Kitamura N, Moriya T, Kuwahara T, Komagiri Y, Toescu EC, Shibuya I. Chronic NGF treatment induces somatic hyperexcitability in cultured dorsal root ganglion neurons of the rat. *Biomed Res* 34: 329–342, 2013. doi:10.2220/biomedres.34.329.

Ke CB, He WS, Li CJ, Shi D, Gao F, Tian YK. Enhanced SCN7A/Nax expression contributes to bone cancer pain by increasing excitability of neurons in dorsal root ganglion. *Neuroscience* 227: 80–89, 2012. doi:10.1016/j.neuroscience.2012.09.046.

Kent AR, Min X, Hogan QH, Kramer JM. Mechanisms of dorsal root ganglion stimulation in pain suppression: a computational modeling analysis. *Neuromodulation* 21: 234–246, 2018. doi:10.1111/ner.12754.

Kim YS, Anderson M, Park K, Zheng Q, Agarwal A, Gong C, Saijilafu, Young L, He S, LaVinka PC, Zhou F, Bergles D, Hanani M, Guan Y, Spray DC, Dong X. Coupled activation of primary sensory neurons contributes to chronic pain. *Neuron* 91: 1085–1096, 2016. doi:10.1016/j.neuron.2016.07.044.

Kiss ZH, Mooney DM, Renaud L, Hu B. Neuronal response to local electrical stimulation in rat thalamus: physiological implications for mechanisms of deep brain stimulation. *Neuroscience* 113: 137–143, 2002. doi:10.1016/S0306-4522(02)00122-7.

Kitamura N, Konno A, Kuwahara T, Komagiri Y. Nerve growth factor-induced hyperexcitability of rat sensory neuron in culture. *Biomed Res* 26: 123–130, 2005. doi:10.2220/biomedres.26.123.

Li Y, North RY, Rhines LD, Tatsui CE, Rao G, Edwards DD, Cassidy RM, Harrison DS, Johansson CA, Zhang H, Dougherty PM. DRG voltage-gated sodium channel 1.7 is upregulated in paclitaxel-induced neuropathy in rats and in humans with neuropathic pain. *J Neurosci* 38: 1124–1136, 2018. doi:10.1523/JNEUROSCI.0899-17.2017.

Liu CN, Wall PD, Ben-Dor E, Michaelis M, Amir R, Devor M. Tactile allodynia in the absence of C-fiber activation: altered firing properties of DRG neurons following spinal nerve injury. *Pain* 85: 503–521, 2000. doi:10.1016/S0304-3959(00)00251-7.

Malsch P, Andratsch M, Vogl C, Link AS, Alzheimer C, Brierley SM, Hughes PA, Kress M. Deletion of interleukin-6 signal transducer gp130 in small sensory neurons attenuates mechanonociception and down-regulates TRPA1 expression. *J Neurosci* 34: 9845–9856, 2014. doi:10.1523/JNEUROSCI.5161-13.2014.

Melemedjian OK, Asiedu MN, Tillu DV, Peebles KA, Yan J, Ertz N, Dussor GO, Price TJ. IL-6- and NGF-induced rapid control of protein synthesis and nociceptive plasticity via convergent signaling to the eIF4F complex. *J Neurosci* 30: 15113–15123, 2010. doi:10.1523/JNEUROSCI.3947-10.2010.

Miller JP, Eldabe S, Buchser E, Johanek LM, Guan Y, Linderoth B. Parameters of spinal cord stimulation and their role in electrical charge delivery: a review. *Neuromodulation* 19: 373–384, 2016. doi:10.1111/ner.12438.

Moy JK, Khoutorsky A, Asiedu MN, Black BJ, Kuhn JL, Barragán-Iglesias P, Megat S, Burton MD, Burgos-Vega CC, Melemedjian OK, Boitano S, Vagner J, Gkogkas CG, Pancrazio JJ, Mogil JS, Dussor G, Sonenberg N, Price TJ. The MNK–eIF4E signaling axis contributes to injury-induced nociceptive plasticity and the development of chronic pain. *J Neurosci* 37: 7481–7499, 2017. doi:10.1523/JNEUROSCI.0220-17.2017.

National Research Council. *Recognition and Alleviation of Pain in Laboratory Animals*. Washington, DC: Nat. Acad. Press, 2009. doi:10.17226/12526.

Newberry K, Wang S, Hoque N, Kiss L, Ahlijanian MK, Herrington J, Graef JD. Development of a spontaneously active dorsal root ganglia assay using multiwell multielectrode arrays. *J Neurophysiol* 115: 3217–3228, 2016. doi:10.1152/jn.01122.2015.

Newton RA, Bingham S, Case PC, Sanger GJ, Lawson SN. Dorsal root ganglion neurons show increased expression of the calcium channel $\alpha 2\delta$-1 subunit following partial sciatic nerve injury. *Brain Res Mol Brain Res* 95: 1–8, 2001. doi:10.1016/S0169-328X(01)00188-7.

Obreja O, Biasio W, Andratsch M, Lips KS, Rathee PK, Ludwig A, Rose-John S, Kress M. Fast modulation of heat-activated ionic current by proinflammatory interleukin 6 in rat sensory neurons. *Brain* 128: 1634–1641, 2005. doi:10.1093/brain/awh490.

Ohara PT, Vit JP, Bhargava A, Romero M, Sundberg C, Charles AC, Jasmin L. Gliopathic pain: when satellite glial cells go bad. *Neuroscientist* 15: 450–463, 2009. doi:10.1177/1073858409336094.

Pearce TM, Wilson JA, Oakes SG, Chiu SY, Williams JC. Integrated microelectrode array and microfluidics for temperature clamp of sensory neurons in culture. *Lab Chip* 5: 97–101, 2005. doi:10.1039/b407871c.

Pfrieger FW, Barres BA. Synaptic efficacy enhanced by glial cells in vitro. *Science* 277: 1684–1687, 1997. doi:10.1126/science.277.5332.1684.

Price TJ, Flores CM. Critical evaluation of the colocalization between calcitonin gene-related peptide, substance P, transient receptor potential vanilloid subfamily type 1 immunoreactivities, and isolectin B_4 binding in primary afferent neurons of the rat and mouse. *J Pain* 8: 263–272, 2007. doi:10.1016/j.jpain.2006.09.005.

Radivojevic M, Jäckel D, Altermatt M, Müller J, Viswam V, Hierlemann A, Bakkum DJ. Electrical identification and selective microstimulation of neuronal compartments based on features of extracellular action potentials. *Sci Rep* 6: 31332, 2016. doi:10.1038/srep31332.

Scholz J, Woolf CJ. The neuropathic pain triad: neurons, immune cells and glia. *Nat Neurosci* 10: 1361–1368, 2007. doi:10.1038/nn1992.

Sleigh JN, Weir GA, Schiavo G. A simple, step-by-step dissection protocol for the rapid isolation of mouse dorsal root ganglia. *BMC Res Notes* 9: 82, 2016. doi:10.1186/s13104-016-1915-8.

Stiefel KM, Englitz B, Sejnowski TJ. Origin of intrinsic irregular firing in cortical interneurons. *Proc Natl Acad Sci USA* 110: 7886–7891, 2013. doi:10.1073/pnas.1305219110.

Study RE, Kral MG. Spontaneous action potential activity in isolated dorsal root ganglion neurons from rats with a painful neuropathy. *Pain* 65: 235–242, 1996. doi:10.1016/0304-3959(95)00216-2.

Suzuki M, Watanabe Y, Oyama Y, Mizuno A, Kusano E, Hirao A, Ookawara S. Localization of mechanosensitive channel TRPV4 in mouse skin. *Neurosci Lett* 353: 189–192, 2003. doi:10.1016/j.neulet.2003.09.041.

Svirskis G, Rinzel J. Influence of temporal correlation of synaptic input on the rate and variability of firing in neurons. *Biophys J* 79: 629–637, 2000. doi:10.1016/S0006-3495(00)76321-1.

Tsantoulas C, Farmer C, Machado P, Baba K, McMahon SB, Raouf R. Probing functional properties of nociceptive axons using a microfluidic culture system. *PLoS One* 8: e80722, 2013. doi:10.1371/journal.pone.0080722.

Ullian EM, Harris BT, Wu A, Chan JR, Barres BA. Schwann cells and astrocytes induce synapse formation by spinal motor neurons in culture. *Mol Cell Neurosci* 25: 241–251, 2004. doi:10.1016/j.mcn.2003.10.011.

Valtcheva MV, Copits BA, Davidson S, Sheahan TD, Pullen MY, McCall JG, Dikranian K, Gereau RW 4th. Surgical extraction of human dorsal root ganglia from organ donors and preparation of primary sensory neuron cultures. *Nat Protoc* 11: 1877–1888, 2016. doi:10.1038/nprot.2016.111.

Veldhuis NA, Bunnett NW. Proteolytic regulation of TRP channels: implications for pain and neurogenic inflammation. *Proc Aust Physiol Soc* 44: 101–108, 2013.

Volkow ND, Collins FS. The role of science in addressing the opioid crisis. *N Engl J Med* 377: 391–394, 2017. doi:10.1056/NEJMsr1706626.

Wang J, Wang XW, Zhang Y, Yin CP, Yue SW. Ca^{2+} influx mediates the TRPV4-NO pathway in neuropathic hyperalgesia following chronic compression of the dorsal root ganglion. *Neurosci Lett* 588: 159–165, 2015. doi:10.1016/j.neulet.2015.01.010.

Wang JG, Strong JA, Xie W, Zhang JM. Local inflammation in rat dorsal root ganglion alters excitability and ion currents in small-diameter sensory neurons. *Anesthesiology* 107: 322–332, 2007. doi:10.1097/01.anes.0000270761.99469.a7.

Watkins LR, Maier SF. Beyond neurons: evidence that immune and glial cells contribute to pathological pain states. *Physiol Rev* 82: 981–1011, 2002. doi:10.1152/physrev.00011.2002.

Waxman SG, Cummins TR, Dib-Hajj S, Fjell J, Black JA. Sodium channels, excitability of primary sensory neurons, and the molecular basis of pain. *Muscle Nerve* 22: 1177–1187, 1999. doi:10.1002/(SICI)1097-4598(199909)22:9<1177::AID-MUS3>3.0.CO;2-P.

White FA, Bhangoo SK, Miller RJ. Chemokines: integrators of pain and inflammation. *Nat Rev Drug Discov* 4: 834–844, 2005. doi:10.1038/nrd1852.

Xiang G, Pan L, Huang L, Yu Z, Song X, Cheng J, Xing W, Zhou Y. Microelectrode array-based system for neuropharmacological applications with cortical neurons cultured in vitro. *Biosens Bioelectron* 22: 2478–2484, 2007. doi:10.1016/j.bios.2006.09.026.

Yang Y, Huang J, Mis MA, Estacion M, Macala L, Shah P, Schulman BR, Horton DB, Dib-Hajj SD, Waxman SG. Nav1.7-A1632G mutation from a family with inherited erythromelalgia: enhanced firing of dorsal root ganglia neurons evoked by thermal stimuli. *J Neurosci* 36: 7511–7522, 2016. doi:10.1523/JNEUROSCI.0462-16.2016.

Zhou YQ, Liu Z, Liu ZH, Chen SP, Li M, Shahveranov A, Ye DW, Tian YK. Interleukin-6: an emerging regulator of pathological pain. *J Neuroinflammation* 13: 141, 2016. doi:10.1186/s12974-016-0607-6.

Zhu W, Oxford GS. Differential gene expression of neonatal and adult DRG neurons correlates with the differential sensitization of TRPV1 responses to nerve growth factor. *Neurosci Lett* 500: 192–196, 2011. doi:10.1016/j.neulet.2011.06.034.